HHS Public Access

Author manuscript

J Am Soc Nephrol. Author manuscript; available in PMC 2024 December 09.

Published in final edited form as:

J Am Soc Nephrol. 2006 April ; 17(4): 956–967. doi:10.1681/ASN.2005111174.

Chloride/Bicarbonate Exchanger SLC26A7 Is Localized in Endosomes in Medullary Collecting Duct Cells and Is Targeted to the Basolateral Membrane in Hypertonicity and Potassium Depletion

Jie Xu[*], **Roger T. Worrell**[†], **Hong C. Li**[*], **Sharon L. Barone**[*], **Snezana Petrovic**[*], **Hassane Amlal**[*], **Manoocher Soleimani**[*,‡]

[*]Department of Medicine, University of Cincinnati, Cincinnati, Ohio

[†]Department of Surgery, University of Cincinnati, Cincinnati, Ohio

[‡]Veterans Affairs Medical Center at Cincinnati, Cincinnati, Ohio

Abstract

SLC26A7 is a Cl^-/HCO_3^- exchanger that is expressed on the basolateral membrane and in the cytoplasm of two distinct acid-secreting epithelial cells: The A-intercalated cells in the kidney outer medullary collecting duct and the gastric parietal cells. The intracellular localization of SLC26A7 suggests the possibility of trafficking between cell membrane and intracellular compartments. For testing this hypothesis, full-length human SLC26A7 cDNA was fused with green fluorescence protein and transiently expressed in MDCK epithelial cells. In monolayer cells in isotonic medium, SLC26A7 showed punctate distribution throughout the cytoplasm. However, in medium that was made hypertonic for 16 h, SLC26A7 was detected predominantly in the plasma membrane. The presence of mitogen-activated protein kinase inhibitors blocked the trafficking of SLC26A7 to the plasma membrane. Double-labeling studies demonstrated the localization of SLC26A7 to the transferrin receptor–positive endosomes. A chimera that was composed of the amino terminal fragment of SLC26A7 and the carboxyl terminal fragment of SLC26A1, and a C-terminal–truncated SLC26A7 were retained in the cytoplasm in hypertonicity. In separate studies, SLC26A7 showed predominant localization in plasma membrane in potassium-depleted isotonic medium (0.5 or 2 mEq/L KCl) *versus* cytoplasmic distribution in normal potassium isotonic medium (4 mEq/L). It is concluded that SLC26A7 is present in endosomes, and its targeting to the basolateral membrane is increased in hypertonicity and potassium depletion. The trafficking to the cell surface suggests novel functional upregulation of SLC26A7 in states that are associated with hypokalemia or increased medullary tonicity. Additional studies are needed to ascertain the role of SLC26A7 in enhanced bicarbonate absorption in outer medullary collecting duct in hypokalemia and in acid-base regulation in conditions that are associated with increased medullary tonicity.

Address correspondence to: Dr. Manoocher Soleimani, Division of Nephrology and Hypertension, Department of Medicine, University of Cincinnati, 231 Albert Sabin Way, MSB 259G, Cincinnati, OH 45267-0585. Fax: 513-558-4309; manoocher.soleimani@uc.edu.

The solute carrier families 4 and 26 (SLC4 and SLC26, respectively) encode two distinct groups of anion exchangers. Several members of the SLC4 family, designated as A1 (SLC4A1~AE1), A2 (SLC4A2~AE2), A3 (SLC4A3~AE3), and A4 (SLC4A9~AE4) are shown to mediate Cl^-/HCO_3^- exchange (1,2). SLC26 is a new family of anion exchangers that is composed of 10 distinct genes (3). Members of the SLC26 family display very specific and limited tissue distribution. Functional studies demonstrate that a number of exchangers from this family, including SLC26A3 (DRA), SLC26A4 (pendrin), SLC26A6 (PAT1 or CFEX), SLC26A7, and SLC26A9 (4-9) mediate Cl^-/HCO_3^- exchange. SLC26A4, A6, and A7 are expressed in the kidney, whereas SLC26A3 and A9 are not. In the kidney, SLC26A4 (pendrin) is expressed on the apical membranes of B-intercalated and non-A non-B–intercalated cells, whereas SLC26A6 (PAT1 or CFEX) is expressed on the brush border membranes of the proximal tubule. In the kidney, pendrin mediates bicarbonate secretion and chloride reabsorption in the connecting segment and cortical collecting duct (5,10-12), whereas PAT1 is involved in transcellular chloride reabsorption in the proximal tubule (6,13-16).

SLC26A7 is a recently cloned member of the SLC26 family (17,18). Functional and molecular studies from our laboratory demonstrated that SLC26A7 is a chloride/bicarbonate exchanger (7). In the stomach, SLC26A7 is expressed on the basolateral membrane of the acid-secreting gastric parietal cells (7), whereas in the kidney, it localizes on the basolateral membrane of acid-secreting A-intercalated (A-IC) cells of the outer medullary collecting duct (OMCD) (8,19). OMCD has the highest rate of acid secretion among the collecting duct segments (20). Proton (acid) secretion across the apical membrane of A-IC cells in OMCD *via* vacuolar H^+-ATPase (and to some extent *via* H^+/K^+ ATPase) results in the generation of intracellular bicarbonate, which will be transported across the basolateral membrane into the peritubular space *via* basolateral Cl^-/HCO_3^- exchanger (20,21). SLC26A7 co-localizes with AE1 (SLC4A1) on the basolateral membrane of A-IC cells of OMCD, indicating possible distinct roles for these two Cl^-/HCO_3^- exchangers in acid secretion and bicarbonate absorption (8,19). A recent study indicated that SLC26A7 can function as a Cl^- channel that is regulated by intracellular pH in the heterologous expression system (22). The reason for the discrepancy between those results and our observations that consistently demonstrate mediation of Cl^-/HCO_3^- exchange by SLC26A7 is currently unclear. The discrepancy may be due in part to the utilization of different expression systems as well as differences in the interpretation of the results. In support of this latter possibility, removal of perfusate chloride resulted in cell alkalinization in SLC26A7-expressing HEK 293 cells (22), an observation that is consistent with SLC26A7's being a Cl^-/HCO_3^- exchanger. Expression of human SLC26A7 in *Xenopus* oocytes increased chloride-dependent cell alkalinization in the presence of CO_2/HCO_3^-, supporting the role of SLC26A7 as a Cl^-/HCO_3^- exchanger (S.L. Alper, Harvard Medical School, personal communication, February 2005).

Our immunofluorescent labeling studies in kidney and stomach demonstrated that in addition to membrane localization, SLC26A7 shows abundant cytoplasmic, submembrane localization, raising the possibility that alteration in trafficking between cell membrane and intracellular compartments may be a major mechanism of functional regulation of this anion exchanger. Toward this end, epitope-tagged SLC26A7 cDNA was expressed in MDCK

epithelial cells that were exposed to hypertonicity or potassium depletion and visualized by confocal microscopy. Our results demonstrate that SLC26A7 is present in recycling endosomes in the cytoplasm in isotonic normal medium but is moved to the membrane in hypertonic or potassium-depleted medium. The significance of the results is discussed.

Materials and Methods

Construction of Epitope-Tagged SLC26A7, C-Terminal–Truncated SLC26A7, Full-Length SLC26A1, and A7/A1 Chimera

The full-length and C-terminal–truncated SLC26A7 were generated by PCR, using the human full-length SLC26A7 DNA (5280 bp and 656 amino acid [aa] residues; Genebank NM_052832). The SLC26A1 (2773 bp and 704 aa residues; Genebank AF349043) and SLC26A7/A1 chimera were generated using mouse cDNA as templates. The resulting wild-type SLC26A7, C-terminal–truncated SLC26A7, SLC26A1, and A7/A1 mutants were amplified and fused translationally in-frame to green fluorescence protein (GFP) by cloning into pcDNA3.1/NT-GFP-TOPO vector (Invitrogen, Carlsbad, CA).

Full-length human SLC26A7 was amplified using the following primers: Primer-237, 5′-GAA ATG ACA GGA GCA AAG AG (sense), and primer-2328, 5′-GTT ATT GTA GCA GAG GTC ATC (antisense). The PCR product was cloned into the GFP fusion TOPO vector (pcDNA3.1/NT-GFP-TOPO vector). This resulted in the expression of GFP-SLC26A7 fusion protein with the GFP fusing to the N-terminus of SLC26A7. Using a similar approach, primer-237, GAA ATG ACA GGA GCA AAG AG (sense), primer-2162, TCA GAT ATG ACT TAT TGC AG (antisense), and primer-1919, TCA TTC TTC ATT GCA GTT G (antisense), were used to generate the SLC26A7-CD16 cDNA, which lacked the last 16 aa residues on the carboxyl terminal end. Full-length mouse SLC26A1 was amplified using the following primers: Primer-22, 5′-GAC AGG ATG GAT GCT TCT C (sense), and primer-2204, 5′-ATT CAC ACC ACT CCT ACA G (antisense) from mouse kidney. The PCR product was cloned into the GFP fusion TOPO vector (pcDNA3.1/NT-GFP-TOPO vector). This resulted in the expression of GFP-SLC26A1 fusion protein with the GFP fusing to the N-terminus of SLC26A1 (GFP-SLC26A1). For generation of A7/A1 chimeras, the amino-terminal end of mouse A7 was fused to the carboxy-terminal end of mouse A1 to generate A7n/A1c chimera, with n and c designating the N-terminal and C-terminal ends, respectively. Toward this end, the DNA fragment encoding aa residues 1 to 473 of mouse SLC26A7 was generated using primers A7–107, AAA ATG ACG GGA GCA AAG AG (sense), and A7–1528, GAA TTC TGG GAA ACG TCC TAA CAC (antisense), and fused in frame to the DNA fragment encoding the aa residues 499 to 705 of mouse SLC26A1 using primers A1, GAATTCTTCTTCTCCCTGCTTAGCCTG (sense), and A1, ATTCACACCACTCCTACAG (antisense). This resulted in the expression of the GFP-SLC26A7/A1 mutant fusion protein, which is composed of the amino-terminal fragment of A7 and the carboxyl terminal fragment of A1.

Transient Expression of Epitope-Tagged SLC26A7, Truncated SLC26A7, SLC26A1, and A7/A1 Mutant in MDCK Cells

MDCK cells were grown on glass coverslips and transiently transfected with the epitope-tagged SLC26 isoforms or variants (above) and studied 48 h later according to established methods (23,24). Briefly, cells were plated in 24-well plates and transfected with various cDNA fragments at 80% confluence using 0.8 μg of DNA and 4 μl of Lipofectamine 2000 (Invitrogen). All cells were co-labeled with Alexa Fluor 568 phalloidin (Molecular Probes, Eugene, OR) as a marker of apical membrane labeling. All cells were fixed 48 h after transfection, irrespective of the duration of exposure to hypertonic or low-potassium medium, such that the total length of exposure to isotonic plus hypertonic or normal-potassium plus low-potassium medium was 48 h.

In separate studies, MDCK cells were grown on permeable polycarbonate membrane Transwell filters (cat. no. 3401; Corning Inc., Corning, NY) at a density of approximately 10^5 cells/cm^2. Cells achieved confluence within 4 to 5 d and then were transiently transfected from the apical surface with the GFP-SLC26A7 construct and studied 48 h later.

Confocal Microscopy and Immunofluorescence Labeling

MDCK cells were washed three times with PBS, fixed for 20 min with 3% formaldehyde in PBS, and washed three more times with PBS. Afterward, cells were permeabilized with 0.1% TX-100 in PBS for 3 min, washed three times with PBS, and co-stained with Alexa Fluor 568 phalloidin. Cells then were washed and mounted on glass slides in Fluoromount-G (Southern Biotechnology Associates, Inc., Birmingham, AL). Images were taken on a Zeiss LSM510 confocal microscope. Both Z-line and Z-stack images were obtained using the LSM 5 Image software to analyze the membrane targeting of GFP-fusion proteins (23,24).

Water Loading in Rats

Sprague-Dawley rats that weighed 150 to 200 g were subjected to water loading for 5 d according to established protocols. Briefly, the control group (n = 4) was allowed tap water *ad libitum,* whereas the water-loaded rats (n = 4) were induced to drink water abundantly by adding glucose (50 g/1000 ml) to their drinking water.

Antibodies

A rabbit polyclonal antibody raised against a mouse SLC26A7 peptide with the aa residues CGAKRKKRSVLWGKMHTP (using the mouse EST with Genbank accession no. BB666404) and an antibody raised against human SLC26A7 were used for immunofluorescence labeling (8,19).

Immunofluorescence Labeling Studies in Mouse Kidney and Stomach

Immunofluorescence labeling was performed as described previously (7,8,19). Alexa Fluor 488 (green) or Alexa Fluor 568 (red) goat anti-rabbit antibody was used as a secondary antibody. Sections were examined on the epifluorescent microscope Eclipse 600 (Nikon Bioscience, Melville, NY) equipped with SPOT digital camera (Diagnostic Instruments,

Inc., Sterling Heights, MI). Digital images were acquired using the Spot Advanced software provided with the camera.

Western Blot Analysis

Microsomal membrane and cytoplasmic fractions were isolated from rat outer medulla according to established methods (25). Immunoblotting experiments were carried out as described previously (8,13). Briefly, the solubilized proteins were size-fractionated on 8% SDS polyacrylamide minigels (Novex, San Diego, CA) under denaturing conditions, electrophoretically transferred to nitrocellulose membranes, blocked with 5% milk proteins, and then probed with the affinity-purified anti-SLC26A7 immune serum at a dilution of 1:400. The secondary antibody was donkey anti-rabbit IgG conjugated to horseradish peroxidase (Pierce, Rockford, IL). The sites of antigen-antibody complex formation on the nitrocellulose membranes were visualized using chemiluminescence method (SuperSignal Substrate; Pierce) and captured on light-sensitive imaging film (Kodak, Rochester, NY).

Materials

All chemicals were purchased from Sigma Chemical Co. (St. Louis, MO). RadPrime DNA labeling kit was purchased from Invitrogen (Carlsbad, CA). mMACHINE kit was purchased from Ambion (Austin, TX). Alexa Fluor–conjugated secondary antibodies and Hoechst 33342 were purchased from Molecular Probes Inc. The CT-GFP fusion expression kit, which contains the pcDNA3.1/CT-GFP TOPO vector, was purchased from Invitrogen. Glyceraldehyde-3-phosphate dehydrogenase polyclonal antibodies were from Abcam (Cambridge, MA).

Statistical Analyses

The experiments were performed in duplicate (two slides per each condition) and repeated at least three separate times for each maneuver. Quantification of SLC26A7 abundance in membrane or cytoplasm was performed using MetaMorph imaging system software (Universal Imaging Corp., West Chester, PA) by measuring the fluorescence intensity of SLC26A7-GFP in multiple square areas corresponding to regions in membrane or cytoplasm. More than 16 separate fields were analyzed per each transfected cell, with the total of 160 fields for 10 transfected cells per each slide. A total of 20 or 30 transfected cells from three separate experiments were analyzed for each maneuver. Values are expressed as arithmetic mean ± SE. Comparisons were done by using unpaired t test, and $P < 0.05$ was considered statistically significant. Microsoft Excel, ProStat (Philscience, South Korea), and PSI-Plot (Philscience) were commercial software packages used for statistical analysis.

Results

Our immunofluorescence labeling with purified antibodies demonstrated the localization of SLC26A7 on the basolateral membrane and in the cytoplasm of parietal cells in the stomach and A-IC cells in kidney OMCD (7,8,19). These results have been confirmed in our new immunofluorescence labeling studies in Figure 1, A and B. Figure 1A shows the subcellular distribution of SLC26A7 in gastric parietal cells when images with gastric H-K-ATPase are merged. Figure 1B shows the subcellular distribution of SLC26A7 in kidney OMCD

cells. The low- and high-magnification images in Figure 1B (left and right, respectively) along with the image in Figure 1A clearly demonstrate the localization of SLC26A7 on the basolateral membrane and in the cytoplasm of acid-secreting gastric parietal cells and OMCD cells.

To verify the cytoplasmic expression of SLC26A7 quantitatively, we performed Western blotting on membrane and cytoplasmic proteins that were isolated from rat outer medulla, the site of SLC26A7 expression. As indicated, Western blotting detected SLC26A7 as an approximately 90-kD band, with abundant expression in both the membrane and the cytoplasmic fractions from two separate rats (Figure 1C, left), confirming the subcellular distribution of the exchanger in the kidney cells. Preadsorption of the antibody with the antigen (synthetic peptide) completely prevented the labeling of SLC26A7 in the kidney outer medulla fractions (Figure 1C, right), indicating the specificity of the antibody.

Expression and Subcellular Distribution of SLC26A7 in MDCK Cells

The cytoplasmic localization of the exchanger in Figure 1 raises the possibility of alteration in SLC26A7 abundance at the cell surface by affecting the trafficking between cell membrane and intracellular compartments. To analyze this possibility, we examined the expression of full-length GFP with or without SLC26A7 cDNA insert in MDCK cells. The cell membrane was labeled with the actin-binding dye phalloidin. Figure 2A is a Z-line merged image of phalloidin and GFP labeling and shows that transfection with GFP vector alone (no SLC26A7 insert) results in the accumulation of GFP in the cytoplasm with no localization on the membrane. It is interesting that when transfection with GFP-SLC26A7 full-length cDNA was performed, the acquired images demonstrated punctate distribution through the cytoplasm, with no labeling on the plasma membrane (Figure 2B).

Effect of Hypertonicity on Distribution of SLC26A7 in MDCK Cells

The expression of SLC26A7 in the kidney is limited predominantly to the medullary collecting duct, a segment that is exposed to a hypertonic environment *in vivo*. The purpose of the next series of experiments was to examine the effect of hypertonicity on subcellular distribution of SLC26A7. Toward this end, cells were transiently transfected with GFP-SLC26A7 cDNA; and 32 h later, the medium was made hypertonic by the addition of 50 mM NaCl. The pH was maintained at 7.4. The cells were fixed for 16 h after switching to the hypertonic medium and analyzed microscopically. As shown in Figure 3A, SLC26A7 was detected predominantly in the plasma membrane, with little residual labeling in the cytoplasm. Analysis of 30 transfected cells in hypertonic medium and 30 cells in isotonic medium by MetaMorph imaging system software (see Materials and Methods) showed that 86 ± 5% of SLC26A7 labeling was detected in the membrane in hypertonic medium, whereas only 13 ± 2% of the labeling was detected in the membrane in isotonic medium ($P < 0.0001$). Subcellular distribution studies in hypertonic medium (Z-stack images) indicate the targeting of SLC26A7 to the basolateral membrane (Figure 3B), consistent with published reports (7,8,19). Transfection with the control construct (empty GFP with no SLC26A7 insert) showed that the GFP was retained in the cytoplasm in hypertonic medium at 2 and 16 h (data not shown) in a manner that was indistinguishable from the isotonic medium (Figure 2A).

The purpose of the next series of experiments was to determine the rapidity with which the shift in SLC26A7 distribution from cytoplasm to the membrane occurs in hypertonic medium. Accordingly, cells were transfected with SLC26A7, switched to the hypertonic medium 46 h later, and fixed for 2 h after switching to the hypertonic medium. As shown in Figure 3C, exposure to the hypertonic medium for 2 h did not significantly increase the abundance of SLC26A7 in the membrane.

The hypertonicity in the above experiments was generated by the addition of 50 mM NaCl. In the next series of experiments, hypertonicity was generated by the addition of sodiumfree solute. Toward this end, mannitol (100 Mm) was added to the medium, and cells were fixed and studied 16 h later. As shown in Figure 3D, SLC26A7 was detected predominantly in the membrane in hypertonic medium. Analysis of 30 transfected cells from three separate experiments showed that 79 ± 5% of SLC26A7 labeling was detected in the membrane after 16 h of incubation with mannitol ($P < 0.0001$, *versus* isotonic medium in Figure 3A).

The above experiments were performed on cells that were grown on nonpermeable support. The next series of experiments were performed in cells that were grown on permeable support (see Materials and Methods). Toward this end, MDCK cells were plated on Transwell filters and transfected with the SLC26A7-GFP construct from the apical surface after becoming confluent. Thirty-two hours after transfection, the medium that faced the basolateral surface, the apical surface, or both surfaces was made hypertonic by the addition of 50 mM NaCl. The cells were fixed for 16 h after switching to the hypertonic medium and analyzed microscopically. As shown in Figure 3E, SLC26A7 was detected predominantly in the cytoplasm in isotonic medium (left) but in the plasma membrane in hypertonic medium added to both the apical and basolateral sides (second panel from left). In cells that were exposed to hypertonic medium from the basolateral side alone (right), the abundance of SLC26A7 in the membrane was similar to that in cells that were exposed to hypertonic medium from both sides (second panel from left). In cells that were exposed to hypertonic medium from the apical surface alone, SLC26A7 was detected predominantly in the cytoplasm with some labeling in the membrane (second panel from right).

In an attempt to identify the signal(s) that mediates the targeting of SLC26A7 to the membrane in hypertonicity, we investigated the role of mitogen-activates protein kinase (MAPK). This assumption was based on published literature demonstrating the activation of MAPK by high osmolarity (26-28). Toward this end, the experiments in hypertonic medium were repeated in the presence or absence of SB203580/S-8307 (Sigma-Aldrich, St. Louis, MO), a specific inhibitor of p38 MAPK (27,28). Accordingly, MDCK cells were transfected with the GFP-SLC26A7 cDNA and then incubated with 10 μM SB203580 upon switching to the hypertonic medium. As shown in Figure 4, the presence of the MAPK inhibitor SB203580 completely blocked the trafficking of SLC26A7 to the membrane (bottom) when compared with its absence (top). Analysis of the epitope-tagged insert in 10 transfected cells with the p38 MAPK inhibitor and 10 cells without the inhibitor in hypertonic medium showed that only 9 ± 2% of SLC26A7 labeling was in the membrane in the presence of the inhibitor *versus* 83 ± 7% in its absence ($P < 0.0001$, three separate experiments). Similarly, addition of PD 98059 (Sigma-Aldrich), an inhibitor of the upstream regulatory protein kinase MAP/extracellular signal–regulated kinase kinase (27,28), also blocked the

trafficking of SLC26A7 to the membrane in hypertonic medium in a manner similar to that shown in Figure 4 (data not shown).

SLC26A7 Resides in Endosomes in MDCK Cells

The disappearance of SLC26A7 from the cytoplasm and its appearance in the plasma membrane in hypertonic medium (Figures 2 and 3) raises the possibility that SLC26A7 may reside in the endosomes. To investigate this possibility, we performed double labeling with SLC26A7-GFP and the transferrin receptor marker (transferrin conjugated with Alexa Fluor 568; Molecular Probes) in both isotonic and hypertonic media. As indicated in Figure 5A, the intracellular localization of GFP-SLC26A7 (right) and transferrin receptor (left) significantly overlapped in isotonic medium. Furthermore, the majority of transferrin receptor (left) and GFP-SLC26A7 (right) labeling was detected in the plasma membrane in hypertonic medium (Figure 5B, merged). Analysis of the epitope-tagged insert in 10 transfected cells in isotonic medium and 10 cells in hypertonic medium from three separate experiments showed significant co-localization of SLC26A7 with the transferrin receptor in hypertonic medium.

Expression of SLC26A1 and SLC26A7/A1 Chimera in MDCK Cells

In the next series of experiments, we examined whether the localization of SLC26A7 in the endosomes is unique to this member of the SLC26 family or is a property that is shared by other members of the SLC26 family. Toward this end, SLC26A1 (also know as SAT1, for sulfate anion transporters 1) (3,16,29) was fused in frame with GFP (see Materials and Methods) and expressed in MDCK cells in isotonic media at pH 7.4. As indicated in Figure 6A, SLC26A1 is expressed predominantly in the plasma membrane, with little expression in the cytoplasm (Z-line image). Subcellular distribution studies in isotonic media (Z-stack image) indicate that SLC26A1 is localized to the basolateral membrane (Figure 6B). The membrane abundance of SLC26A1 did not change in hypertonic medium (data not shown). These studies support the conclusion that the pattern of distribution of SLC26A7 is unique to this isoform and does not extend to other members of the SLC26 family.

Next, we examined the expression of the SLC26A7/A1 mutant, which encoded the N-terminal portion of A7 and the C-terminal fragment of A1 in isotonic and hypertonic media (see Materials and Methods). The results demonstrate that A7/A1 chimera is localized predominantly to the cytoplasm in isotonic medium (Figure 6C, left) and shows little expression in the membrane in hypertonic medium (Figure 6C, right). Analysis of 20 transfected cells in hypertonic or isotonic medium (see Materials and Methods) showed that 79 ± 7% of SLC26A7 labeling in isotonic medium and 69 ± 6% in hypertonic medium was detected in the cytoplasm ($P > 0.05$). These results suggest that the signal that directs the targeting of SLC26A7 to the membrane in hypertonic medium likely resides in the C-terminal end of SLC26A7. It is worth mentioning that mouse SLC26A7, which was used for domain-swapping experiments in Figure 6, shows a subcellular distribution pattern similar to the human SLC26A7 (data not shown), indicating that species difference does not play any role in membrane targeting of SLC26A7.

Expression of C-Terminal–Truncated SLC26A7 in MDCK Cells

In the next series of experiments, the expression of the truncated SLC26A7 (see Materials and Methods) was examined in isotonic medium and hypertonic medium. As indicated in Figure 6D (left), deletion of the last 16 aa residues from the C-terminal end resulted in a more diffuse intracellular distribution with little expression in the membrane (Z-line image). The truncated SLC26A7 was retained predominantly in the cytoplasm with faint labeling in the plasma membrane in hypertonic medium (Figure 6D, right). Analysis of 20 transfected cells in hypertonic or isotonic medium showed that 81 ± 6% of SLC26A7 labeling in isotonic medium and 74 ± 7% in hypertonic medium was detected in the cytoplasm ($P > 0.05$). Taken together, these data indicate that a domain within the last 16 aa of the C-terminal fragment is responsible for the targeting of SLC26A7 to the membrane in hypertonic medium.

Effect of Potassium Depletion on Expression GFP-SLC26A7 in MDCK Cells

Rats that are fed a potassium-free diet for 3 to 7 d demonstrate increased bicarbonate reabsorption in their OMCD (30), suggesting the upregulation of apical and basolateral bicarbonate-absorbing transporters in A-IC cells (31). On the basis of the studies showing the localization of SLC26A7 to the basolateral membrane of A-IC cells in OMCD (8,19), we entertained the possibility that potassium depletion might regulate the trafficking of SLC26A7 to the membrane. Toward this end, cells were transiently transfected with GFP-SLC26A7 cDNA and thereafter were exposed to either very low potassium (0.5 mM/L) or low potassium (2 mM/L) and compared with normal potassium (4 mEq/L) for 16 or 2 h. The medium was kept isotonic with all potassium concentrations. Figure 7 compares the effect of varying potassium concentration on subcellular distribution of GFP-SLC26A7. As indicated, SLC26A7 was detected predominantly in the plasma membrane in very-low-potassium medium (0.5 mM) for 16 h (right) *versus* in punctate cytoplasmic structures in normal-potassium medium (left). At 2 mM potassium for 16 h, SLC26A7 shows significant abundance in the membrane *versus* the isotonic medium, with moderate cytoplasmic localization (second panel from right) when compared with 0.5 mEq/L potassium (right). The abundance of SLC26A7 in the membrane was estimated at approximately 23 ± 4% in normal potassium, 58 ± 5% in 2 mEq/L potassium ($P < 0.001$ *versus* normal-potassium medium), and 81 ± 5% in 0.5 mEq/L potassium for 16 h ($P < 0.0001$ *versus* normal-potassium medium), with a total of 30 cells analyzed for each potassium concentration. A shorter exposure of MDCK cells (2 h) to low-potassium medium (2 mEq/L) did not increase the membrane abundance of SLC26A7 (Figure 7, second panel from left). Transfection with the control construct (empty GFP with no SLC26A7 insert) showed that the GFP was retained in the cytoplasm in low-potassium medium at 2 and 16 h (data not shown) in a manner that was indistinguishable from the normal medium (Figure 2A).

SLC26A7 Expression in Water-Loaded Rats

The results of the experiments in Figures 2, 3, and 4 as well as a recently published report (32) demonstrate that increased interstitial tonicity increases, whereas decreased interstitial tonicity decreases the membrane abundance of SLC26A7 in OMCD cells. To examine the effect of reduced interstitial osmolarity on SLC26A7 in a more detailed manner, we

subjected rats to water loading for 5 d (see Materials and Methods) and then examined them by immunofluorescence labeling. Water-loaded rats displayed significant polyuria (increased urine output) and reduced urine osmolarity *versus* control rats, consistent with published reports. As demonstrated in low- and high-magnification images of the kidney outer medulla (Figure 8, top and bottom, respectively), the number of OMCD cells that displayed SLC26A7 expression on their basolateral membrane decreased significantly in water-loaded rats (Figure 8, right) *versus* normal control rats (Figure 8, left). The reduction in membrane expression was associated with a reciprocal increase in SLC26A7 abundance in the cytoplasm in OMCD cells (Figure 8).

Discussion

Immunocytochemical staining (7,8,19) as well as immunoblot analysis (Figure 1) demonstrated that in addition to basolateral membrane, significant intracellular localization of SLC26A7 is observed in kidney medullary collecting or gastric parietal cells, raising the possibility that alteration in SLC26A7 abundance at the cell surface may occur by changes in traffic between cell membrane and intracellular compartments. Epitopetagged full-length human SLC26A7 was detected predominantly as punctate distribution in the cytoplasm (Figure 2). However, in hypertonic medium (50 mM NaCl or 100 mM mannitol added to the isotonic medium [pH 7.4]), SLC26A7 appeared predominantly on the plasma membrane (Figure 3). The presence of MAPK inhibitors completely blocked the trafficking of SLC26A7 to the plasma membrane (Figure 4). Double labeling with the transferrin receptor markers demonstrated that SLC26A7 shows significant expression in recycling endosomes (Figure 5). The signal directing the trafficking of SLC26A7 between endosomes and the plasma membrane resides in its C-terminal end (Figure 6). Last, we observe that SLC26A7 was detected predominantly in plasma membrane in potassium-depleted medium *versus* cytoplasmic localization in normal-potassium media (Figure 7). The trafficking to the membrane in hypertonic or potassium-depleted medium was time dependent. Water loading, which decreases the medullary interstitial osmolality, decreased the membrane abundance of SLC26A7 (Figure 8).

The detection of SLC26A7 in the plasma membrane of cells that were exposed to hypertonic medium *in vitro* suggests that alterations in kidney medullary interstitial osmolarity *in vivo* can affect the abundance of SLC26A7 in the basolateral membrane of A-IC cells in OMCD. In support of this possibility, studies in Brattleboro rats, which lack endogenous vasopressin and, as a result, have reduced medullary interstitial osmolarity (33,34), showed very little SLC26A7 expression on the basolateral membrane of medullary collecting duct cells (32). It is interesting that treatment with vasopressin, which normalizes the medullary interstitial osmolarity (33,34), resulted in significant upregulation of SLC26A7 on the basolateral membrane of OMCD cells without affecting its mRNA expression levels (32). These results are consistent with posttranscriptional regulation of SLC26A7 by vasopressin in Brattleboro rats and are in agreement with enhanced trafficking of SLC26A7 to the membrane by hypertonicity *in vitro* (Figures 3, 4, and 5). In contrast to SLC26A7, AE1 is abundantly expressed in the basolateral membrane of A-IC in OMCD in Brattleboro rats, and its expression actually decreases, albeit very mildly, in response to vasopressin (32). The robust

SLC26A7 appearance in basolateral membranes and its distinct response *versus* AE1 to vasopressin suggest differential regulation of AE1 and SLC26A7 in pathophysiologic states.

A recent report showed that in rats that were subjected to water deprivation for 3 d, the mRNA and protein expression of SLC26A7 in OMCD were enhanced (19). The transcriptional regulation of SLC26A7 in water deprivation does not conflict with its posttranscriptional regulation by hypertonicity in cultured medullary collecting duct cells *in vitro* (Figures 3, 4, and 5) or by vasopressin in Brattleboro rats (32). It is plausible that increased interstitial tonicity of medulla can increase the expression of SLC26A7 at both transcriptional and posttranscriptional levels, with transcriptional regulation becoming the dominant regulatory mode at longer duration or more severe degree of hypertonicity such as 3 d of water deprivation. Alternatively, it is possible that the transcriptional regulation of SLC26A7 in water deprivation is due to factors other than increased medullary osmolarity such as volume depletion, activation of renin angiotensin and sympathetic systems, or decreased kidney perfusion, (35,36).

The trafficking of ion transporters, in particular acid-base transporters such as H^+-ATPase, between intracellular structures and the plasma membrane has been well described (37-39). However, unlike these ion transporters, the trafficking of SLC26A7 to the membrane is slow and time dependent (Figures 3 and 4). As a Cl^-/HCO_3^- exchanger that is adapted to hypertonicity, SLC26A7 activation results in the entry of chloride, which subsequently regulates cell volume. In this regard, SLC26A7 function may be similar to betaine transporter, which is involved in cell volume regulation and shows a time-dependent trafficking in hypertonicity that is very similar to SLC26A7 (40). The bicarbonate exit that is coupled to chloride entry suggests that SLC26A7, which exchanges chloride for bicarbonate across the basolateral membrane of acid-secreting OMCD cells, will also regulate cell pH and/or bicarbonate exit in hypertonicity in a time-dependent manner. The lack of acute regulation of SLC26A7 in hypertonicity suggests either that AE1, which co-localizes with SLC26A7, is not acutely inhibited by hypertonicity or that other acid-base transporters may be activated immediately after the generation of hypertonicity.

The localization of SLC26A7 in the endosomes is unique among SLC26 members. SLC26A1 (SAT1) was expressed predominantly on the basolateral membrane of MDCK cells in isotonic medium (Figure 6, B and C) and remained in the membrane in hypertonic medium (data not shown). Furthermore, our preliminary studies demonstrate that epitope-tagged AE1, which co-localizes with SLC26A7 on the basolateral membrane of cells in OMCD (8,19), is expressed predominantly in plasma membrane in MDCK cells in isotonic medium (data not shown), confirming published reports (41). Taken together, these results suggest that SLC26A7 trafficking is distinct from SLC4A1 and other SLC26 anion exchangers.

The targeting of SLC26A7 to the membrane was completely prevented in the presence of MAPK inhibitors (Figure 4), indicating that MAPK is activated and plays an important role in enhanced cell surface expression of SLC26A7 in a hypertonic environment. These findings are consistent with published reports indicating that hypertonicity increases the membrane targeting and/or activity of several ion transporters, including Na-K-AT-Pase,

Glut 4, and AE2 (42-44). Whether the activation of MAPK is in response to the hypertonicity or the consequent cell shrinkage remains speculative (27,28). Authors could not find any published studies in mammalian cells demonstrating a critical role for MAPK in the alteration in endosomal/surface membrane trafficking of acid-base transporters in a high osmotic environment. As such, these results may be the first report on such finding. Furthermore, whereas the trafficking of the recycling endosomes to the membrane has been demonstrated in acute hypertonicity, little information is available regarding their targeting to the membrane in long-term (16 h) hypertonicity. In addition to blocking membrane targeting, p38 MAPK inhibitor seemed to reduce the overall signal intensity of SLC26A7, suggesting a possible effect on its abundance (Figure 4). Whether MAPK inhibitors directly reduce the synthesis of new SLC26A7 protein remains speculative. A more plausible explanation is that the SLC26A7 protein that is destined for the plasma membrane undergoes enhanced degradation in the lysosomes after being retained in the cytoplasm.

The truncated SLC26A7, lacking the last 16 aa, showed a distribution pattern that was very distinct from the full-length protein in isotonic and hypertonic media (Figure 6, A and B). Similar to the truncated SLC26A7, the A7/A1 chimera was expressed diffusely in the cytoplasm in isotonic medium and showed little membrane expression in hypertonic medium (Figure 6D). These latter experiments confirm the results of the studies with the C-terminal–truncated mutant and suggest that the determinant site that directs the trafficking of SLC26A7 from the recycling endosomes to the membrane resides in its C-terminal end. Future studies should focus on the identification of the aa residues that are responsible for the targeting of SLC26A7 to the endosomes and its trafficking to the membrane in pathophysiologic states.

Potassium depletion causes metabolic alkalosis in mammals (45,46), in large part as a result of increased absorption of bicarbonate in the kidney proximal tubule and the collecting duct (30,31,47,48). Rats that were fed a potassium-free diet developed significant hypokalemia or intracellular potassium depletion as early as 24 h after ingestion of the diet (49). *In vitro* microperfusion studies in the collecting duct demonstrated increased absorption of bicarbonate in OMCD in rats that were fed a potassium-free diet for 7 d (30). Molecular studies demonstrated increased abundance of apical H+-ATPase and colonic H+-K+-ATPase in OMCD of potassium-depleted rats and mice (50,51). However, the identity of the basolateral Cl^-/ HCO_3^- exchanger in the OMCD cells that is upregulated in potassium depletion, whether SLC26A7 or AE1, remained and still remains speculative. These results demonstrate that SLC26A7 abundance in the membrane was increased significantly in potassium-depleted medium (Figure 7). On the basis of our *in vitro* experiments, we propose that potassium depletion increases the abundance of SLC26A7 in basolateral membrane of rat OMCD *in vivo*, thereby increasing net bicarbonate absorption in hypokalemia.

Conclusion

SLC26A7 displays unique subcellular distribution in kidney cells, with predominant abundance in endosomes in normal-potassium isotonic medium and almost exclusive detection in the membrane in either hypertonic or potassium-depleted medium. The

trafficking to the cell surface suggests novel functional upregulation of SLC26A7 in states that are associated with increased medullary tonicity or hypokalemia. Additional studies in pathophysiologic conditions in rats and more specifically in genetically engineered mice that lack SLC26A7 should clarify the role of SLC26A7 in enhanced bicarbonate absorption in OMCD in hypokalemia and in acid-base regulation in conditions that are associated with increased medullary tonicity.

Acknowledgments

These studies were supported by National Institutes of Health grant DK 62809, a Merit Review Grant, a Cystic Fibrosis Foundation grant, and grants from Dialysis Clinic Incorporated (to M.S.).

References

1. Alper SL, Darman RB, Chernova MN, Dahl NK: The AE gene family of Cl/HCO3− exchangers. J Nephrol 15[Suppl 5]: S41–S53, 2002 [PubMed: 12027221]
2. Soleimani M, Burnham CE: Na+ :HCO(3−) cotransporters (NBC): Cloning and characterization. J Membr Biol 183: 71–84, 2001 [PubMed: 11562789]
3. Mount DB, Romero MF: The SLC26 gene family of multifunctional anion exchangers. Pflugers Arch 447: 710–721, 2004 [PubMed: 12759755]
4. Melvin JE, Park K, Richardson L, Schultheis PJ, Shull GE: Mouse down-regulated in adenoma (DRA) is an intestinal Cl(−)/HCO(3)(−) exchanger and is up-regulated in colon of mice lacking the NHE3 Na(+)/H(+) exchanger. J Biol Chem 274: 22855–22861, 1999 [PubMed: 10428871]
5. Soleimani M, Greeley T, Petrovic S, Wang Z, Amlal H, Kopp P, Burnham CE: Pendrin: An apical Cl−/OH−/HCO3− exchanger in the kidney cortex. Am J Physiol Renal Physiol 280: F356–F364, 2001 [PubMed: 11208611]
6. Wang Z, Petrovic S, Mann E, Soleimani M: Identification of an apical Cl(−)/HCO3(−) exchanger in the small intestine. Am J Physiol Gastrointest Liver Physiol 282: G573–G579, 2002 [PubMed: 11842009]
7. Petrovic S, Ju X, Barone S, Seidler U, Alper SL, Lohi H, Kere J, Soleimani M: Identification of a basolateral Cl−/HCO3− exchanger specific to gastric parietal cells. Am J Physiol Gastrointest Liver Physiol 284: G1093–G1103, 2003 [PubMed: 12736153]
8. Petrovic S, Barone S, Xu J, Conforti L, Ma L, Kujala M, Kere J, Soleimani M: SLC26A7: A basolateral Cl−/HCO3− exchanger specific to intercalated cells of the outer medullary collecting duct. Am J Physiol Renal Physiol 286: F161–F169, 2004 [PubMed: 12965893]
9. Xu J, Henriksnas J, Barone S, Witte D, Shull GE, Forte JG, Holm L, Soleimani M: SLC26A9 is expressed in gastric surface epithelial cells, mediates Cl−/HCO3− exchange, and is inhibited by NH4+. Am J Physiol Cell Physiol 289: C493–C505, 2005 [PubMed: 15800055]
10. Royaux IE, Wall SM, Karniski LP, Everett LA, Suzuki K, Knepper MA, Green ED: Pendrin, encoded by the Pendred syndrome gene, resides in the apical region of renal intercalated cells and mediates bicarbonate secretion. Proc Natl Acad Sci U S A 98: 4221–4226, 2001 [PubMed: 11274445]
11. Wall SM, Hassell KA, Royaux IE, Green ED, Chang JY, Shipley GL, Verlander JW: Localization of pendrin in mouse kidney. Am J Physiol Renal Physiol 284: F229–F241, 2003 [PubMed: 12388426]
12. Wagner CA, Finberg KE, Stehberger PA, Lifton RP, Giebisch GH, Aronson PS, Geibel JP: Regulation of the expression of the Cl−/anion exchanger pendrin in mouse kidney by acid-base status. Kidney Int 62: 2109–2117, 2002 [PubMed: 12427135]
13. Knauf F, Yang CL, Thomson RB, Mentone SA, Giebisch G, Aronson PS: Identification of a chloride-formate exchanger expressed on the brush border membrane of renal proximal tubule cells. Proc Natl Acad Sci U S A 98: 9425–9430, 2001 [PubMed: 11459928]

14. Wang Z, Wang T, Petrovic S, Tuo B, Riederer B, Barone S, Lorenz JN, Seidler U, Aronson PS, Soleimani M: Renal and intestinal transport defects in Slc26a6-null mice. Am J Physiol Cell Physiol 288: C957–C965, 2005 [PubMed: 15574486]
15. Petrovic S, Ma L, Wang Z, Soleimani M: Identification of an apical Cl−/HCO3− exchanger in rat kidney proximal tubule. Am J Physiol Cell Physiol 285: C608–C617, 2003 [PubMed: 12736136]
16. Xie Q, Welch R, Mercado A, Romero MF, Mount DB: Molecular characterization of the murine Slc26a6 anion exchanger: Functional comparison with Slc26a1. Am J Physiol Renal Physiol 283: F826–F838, 2002 [PubMed: 12217875]
17. Lohi H, Kujala M, Makela S, Lehtonen E, Kestila M, Saarialho-Kere U, Markovich D, Kere J: Functional characterization of three novel tissue-specific anion exchangers SLC26A7, -A8, and -A9. J Biol Chem 277:14246–14254, 2002 [PubMed: 11834742]
18. Vincourt JB, Jullien D, Kossida S, Amalric F, Girard JP: Molecular cloning of SLC26A7, a novel member of the SLC26 sulfate/anion transporter family, from high endothelial venules and kidney. Genomics 79: 249–256, 2002 [PubMed: 11829495]
19. Barone S, Amlal H, Xu J, Kujala M, Kere J, Petrovic S, Soleimani M: Differential regulation of basolateral Cl−/HCO3− exchangers SLC26A7 and AE1 in kidney outer medullary collecting duct. J Am Soc Nephrol 15: 2002–2011, 2004 [PubMed: 15284286]
20. Schuster VL: Function and regulation of collecting duct intercalated cells. Annu Rev Physiol 55: 267–288, 1993 [PubMed: 8466177]
21. Weiner ID, Wingo CS, Hamm LL: Regulation of intracellular pH in two cell populations of inner stripe of rabbit outer medullary collecting duct. Am J Physiol 265: F406–F415, 1993 [PubMed: 8214100]
22. Kim KH, Shcheynikov N, Wang Y, Muallem S: SLC26A7 is a Cl− channel regulated by intracellular pH. J Biol Chem 280: 6463–6470, 2005 [PubMed: 15591059]
23. Li HC, Worrell RT, Matthews JB, Husseinzadeh H, Neumeier L, Petrovic S, Conforti L, Soleimani M: Identification of a carboxyl-terminal motif essential for the targeting of Na+-HCO3− cotransporter NBC1 to the basolateral membrane. J Biol Chem 279: 43190–43197, 2004 [PubMed: 15273250]
24. Li HC, Szigligeti P, Worrell RT, Matthews JB, Conforti L, Soleimani M: Missense mutations in Na+ :HCO3− cotransporter NBC1 show abnormal trafficking in polarized kidney cells: A basis of proximal renal tubular acidosis. Am J Physiol Renal Physiol 289: F61–F71, 2005 [PubMed: 15713912]
25. Kim SW, Kim JW, Choi KC, Ma SK, Oh Y, Jung JY, Kim J, Lee J: Indomethacin enhances shuttling of aquaporin-2 despite decreased abundance in rat kidney. J Am Soc Nephrol 15: 2998–3005, 2004 [PubMed: 15579502]
26. Wojtaszek PA, Heasley LE, Berl T: In vivo regulation of MAP kinases in *Ratus norvegicus* renal papilla by water loading and restriction. J Clin Invest 102: 1874–1881, 1998 [PubMed: 9819374]
27. Roger F, Martin PY, Rousselot M, Favre H, Feraille E: Cell shrinkage triggers the activation of mitogen-activated protein kinases by hypertonicity in the rat kidney medullary thick ascending limb of the Henle's loop. Requirement of p38 kinase for the regulatory volume increase response. J Biol Chem 274: 34103–34110, 1999 [PubMed: 10567379]
28. Sheikh-Hamad D, Di Mari J, Suki WN, Safirstein R, Watts BA 3rd, Rouse D: p38 kinase activity is essential for osmotic induction of mRNAs for HSP70 and transporter for organic solute betaine in Madin-Darby canine kidney cells. J Biol Chem 273: 1832–1837, 1998 [PubMed: 9430735]
29. Lee A, Beck L, Markovich D: The mouse sulfate anion transporter gene Sat1 (Slc26a1): Cloning, tissue distribution, gene structure, functional characterization, and transcriptional regulation thyroid hormone. DNA Cell Biol 22: 19–31, 2003 [PubMed: 12590734]
30. Nakamura S, Wang Z, Galla JH, Soleimani M: K+ depletion increases. Am J Physiol 274: F687–F692, 1998 [PubMed: 9575892]
31. Wingo CS: Active proton secretion and potassium absorption in the rabbit outer medullary collecting duct. Functional evidence for proton-potassium-activated adenosine triphosphatase. J Clin Invest 84: 361–365, 1989 [PubMed: 2544629]

32. Petrovic S, Amlal H, Ma L, Sun X, Karet F, Barone S, Soleiman M: Vasopressin induces the expression of the Cl−/HCO3− exchanger SLC26A7 in the kidney medullary collecting duct of Brattleboro rats. Am J Physiol Renal Physiol 2006, in press
33. Blumenfeld JD, Hebert SC, Heilig CW, Balschi JA, Stromski ME, Gullans SR: Organic osmolytes in inner medulla of Brattleboro rat: Effects of ADH and dehydration. Am J Physiol 256: F916–F922, 1989 [PubMed: 2719121]
34. DiGiovanni SR, Nielsen S, Christensen EI, Knepper MA: Regulation of collecting duct water channel expression by vasopressin in Brattleboro rat. Proc Natl Acad Sci U S A 91: 8984–8988, 1994 [PubMed: 7522327]
35. Bird JE, Blantz RC: Acute renal failure: The glomerular and tubular connection. Pediatr Nephrol 1: 348–358, 1987 [PubMed: 3153299]
36. Ishikawa E: Experimental study of effect of water deprivation-induced dehydration on renal function in rats. Hinyokika Kiyo 33: 1342–1348, 1987 [PubMed: 3434489]
37. Sautin YY, Lu M, Gaugler A, Zhang L, Gluck SL: Phosphatidylinositol 3-kinase-mediated effects of glucose on vacuolar H+-ATPase assembly, translocation, and acidification of intracellular compartments in renal epithelial cells. Mol Cell Biol 25: 575–589, 2005 [PubMed: 15632060]
38. Brown D, Breton S: H(+)V-ATPase-dependent luminal acidification in the kidney collecting duct and the epididymis/vas deferens: Vesicle recycling and transcytotic pathways. J Exp Biol 203: 137–145, 2000 [PubMed: 10600682]
39. Thurmond DC, Ceresa BP, Okada S, Elmendorf JS, Coker K, Pessin JE: Regulation of insulin-stimulated GLUT4 translocation by Munc18c in 3T3L1 adipocytes. J Biol Chem 273: 33876–33883, 1998 [PubMed: 9837979]
40. Kempson SA, Parikh V, Xi L, Chu S, Montrose MH: Subcellular redistribution of the renal betaine transporter during hypertonic stress. Am J Physiol Cell Physiol 285: C1091–C1100, 2003 [PubMed: 12839828]
41. Beckmann R, Toye AM, Smythe JS, Anstee DJ, Tanner MJ: An N-terminal GFP tag does not alter the functional expression to the plasma membrane of red cell and kidney anion exchanger (AE1) in mammalian cells. Mol Membr Biol 19: 187–200, 2002 [PubMed: 12463718]
42. Chernova MN, Stewart AK, Jiang L, Friedman DJ, Kunes YZ, Alper SL: Structure-function relationships of AE2 regulation by Ca(i)(2+)-sensitive stimulators NH(4+) and hypertonicity. Am J Physiol Cell Physiol 284: C1235–C1246, 2003 [PubMed: 12529246]
43. Randhawa VK, Thong FS, Lim DY, Li D, Garg RR, Rudge R, Galli T, Rudich A, Klip A: Insulin and hypertonicity recruit GLUT4 to the plasma membrane of muscle cells by using N-ethylmaleimide-sensitive factor-dependent SNARE mechanisms but different v-SNAREs: Role of TI-VAMP. Mol Biol Cell 15: 5565–5573, 2004 [PubMed: 15469990]
44. Pihakaski-Maunsbach K, Tokonabe S, Vorum H, Rivard CJ, Capasso JM, Berl T, Maunsbach AB: The gamma-subunit of Na-K-ATPase is incorporated into plasma membranes of mouse IMCD3 cells in response to hypertonicity. Am J Physiol Renal Physiol 288: F650–F657, 2005 [PubMed: 15572522]
45. Hulter HN, Sigala JF, Sebastian A: K+ deprivation potentiates the renal alkalosis-producing effect of mineralocorticoid. Am J Physiol 235: F298–F309, 1978 [PubMed: 29494]
46. Alpern RJ, Emmett M, Seldin DW: Metabolic alkalosis. In: The Kidney: Physiology and Pathophysiology, 2nd Ed., edited by Seldin DW, Giebish G, New York, Raven Press, 1992, pp 2733–2756
47. Kunau RT Jr, Frick A, Rector FC Jr, Seldin DW: Micropuncture study of the proximal tubular factors responsible for the maintenance of alkalosis during potassium deficiency in the rat. Clin Sci 34: 223–231, 1968 [PubMed: 5653684]
48. Soleimani M, Bergman JA, Hosford MA, McKinney TD: Potassium depletion increases luminal Na+/H+ exchange and basolateral Na+:CO3−:HCO3− cotransport in rat renal cortex. J Clin Invest 86: 1076–1083, 1990 [PubMed: 2170445]
49. Amlal H, Krane CM, Chen Q, Soleimani M: Early polyuria and urinary concentrating defect in potassium deprivation. Am J Physiol Renal Physiol 279: F655–F663, 2000 [PubMed: 10997915]
50. DuBose TD Jr, Codina J, Burges A, Pressley TA: Regulation of H(+)-K(+)-ATPase expression in kidney. Am J Physiol 269: F500–F507, 1995 [PubMed: 7485534]

51. Silver RB, Soleimani M: H+-K+-ATPases: Regulation and role in pathophysiological states. Am J Physiol 276: F799–F811, 1999 [PubMed: 10362769]

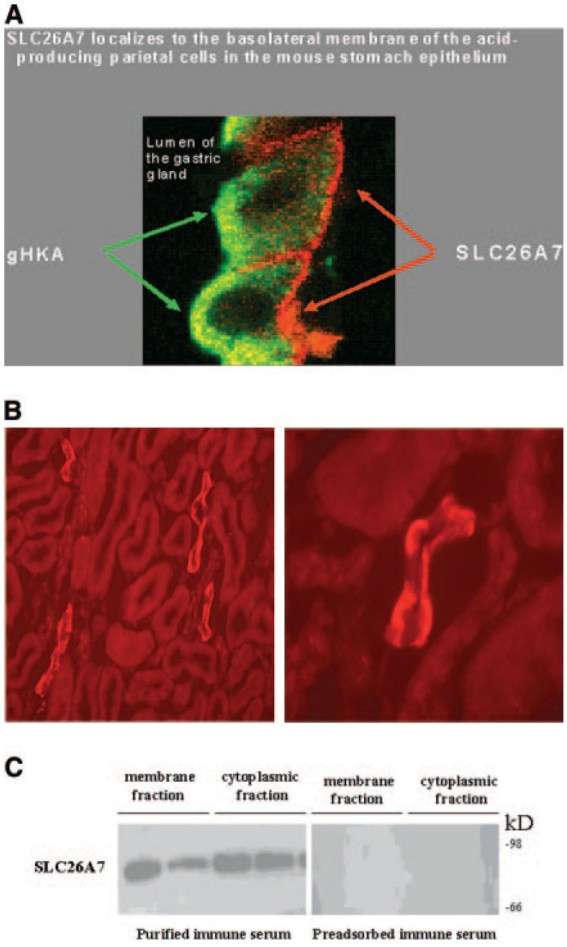

Figure 1.

SLC26A7 expression in mouse kidney outer medullary collecting duct (OMCD) and stomach parietal cells. (A) Immunofluorescence labeling of SLC26A7 and gastric H-K-ATPase in gastric parietal cells. Merged image of SLC26A7 and gastric H-K-ATPase labeling is shown. As indicated, SLC26A7 shows significant intracellular as well as basolateral membrane localization in gastric parietal cells. (B) Immunofluorescence labeling of SLC26A7 in kidney outer medulla. SLC26A7 shows labeling on the basolateral membrane as well as in the cytoplasm in a subpopulation of OMCD cells (left, low magnification; right, high magnification). (C) Immunoblotting of SLC26A7 in membrane and cytoplasmic fractions in kidney outer medulla. Microsomal membranes and cytoplasmic fractions from outer medulla of two rat kidneys were loaded at 100 μg/lane onto lanes. Immunoblotting with the purified immune serum shows a band with a molecular weight of approximately 90 kD in both the membrane and cytoplasmic fractions (left). The labeling of the 90-kD band was abolished with preadsorbed immune serum in both fractions (right).

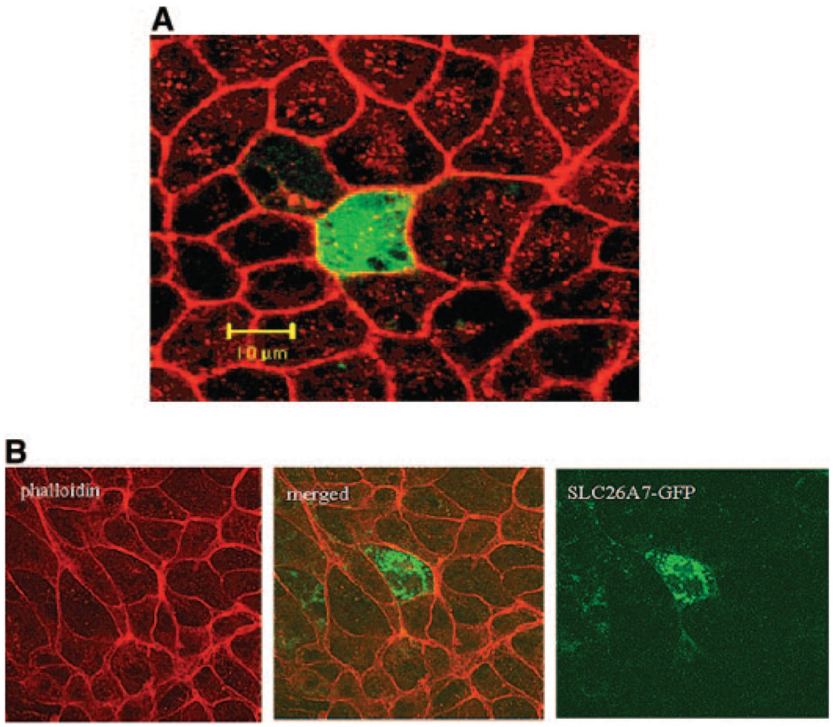

Figure 2.

Expression and subcellular distribution of green fluorescence protein (GFP)-SLC26A7 in MDCK cells. (A) Transfection with GFP vector alone (no SLC26A7 insert) results in GFP accumulation in the cytoplasm (Z-line images). (B) GFP-SLC26A7 is expressed in punctate cytoplasmic structures, with no labeling on the membrane. Red, phalloidin; green, GFP.

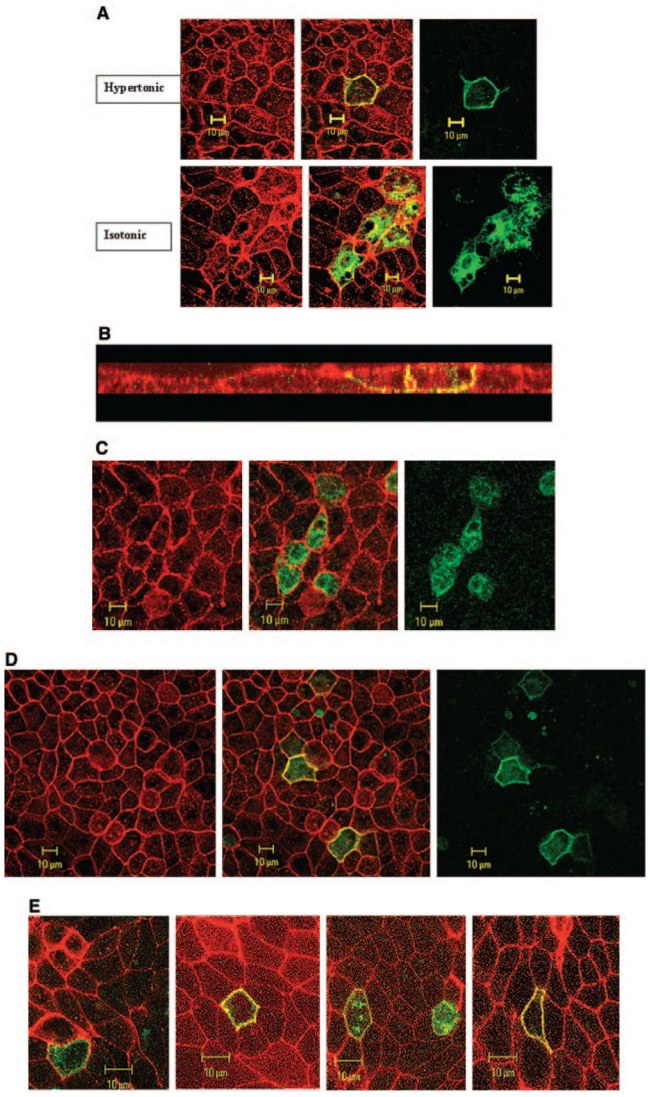

Figure 3.

Effect of hypertonicity on the expression and subcellular distribution of SLC26A7 in MDCK cells. (A) Expression of SLC26A7 in hypertonic medium (top) *versus* isotonic medium (bottom). As shown, SLC26A7 was detected almost exclusively in the plasma membrane in hypertonic medium (top) *versus* predominantly in intracellular compartments in isotonic medium (bottom). Red, phalloidin; green, SLC26A7-GFP. (B) Subcellular distribution studies in hypertonic medium. Merged Z-stack image of GFP-SLC26A7 and phalloidin indicates the targeting of SLC26A7 to the basolateral membrane. (C) Effect of 2 h of exposure to hypertonic medium on SLC26A7 distribution in MDCK cells. As shown, SLC26A7 was detected predominantly in the cytoplasm after 2 h of incubation in hypertonic medium. Red, phalloidin; green, SLC26A7-GFP. (D) Effect of mannitol on SLC26A7 distribution in MDCK cells. As shown, SLC26A7 was detected predominantly in the membrane after 16 h of incubation in hypertonic medium. Red, phalloidin; green, SLC26A7-GFP. (E) SLC26A7 expression in cells that were grown on permeable support. As shown, cells that were grown on permeable support were detected predominantly in the

cytoplasm in isotonic medium. However, in cells that were exposed to hypertonic medium from the basolateral and apical surfaces or from the basolateral surface alone, SLC26A7 was detected predominantly on the plasma membrane. When hypertonicity was applied to the apical surface alone, SLC26A7 showed mild abundance in the membrane with significant retention in the cytoplasm.

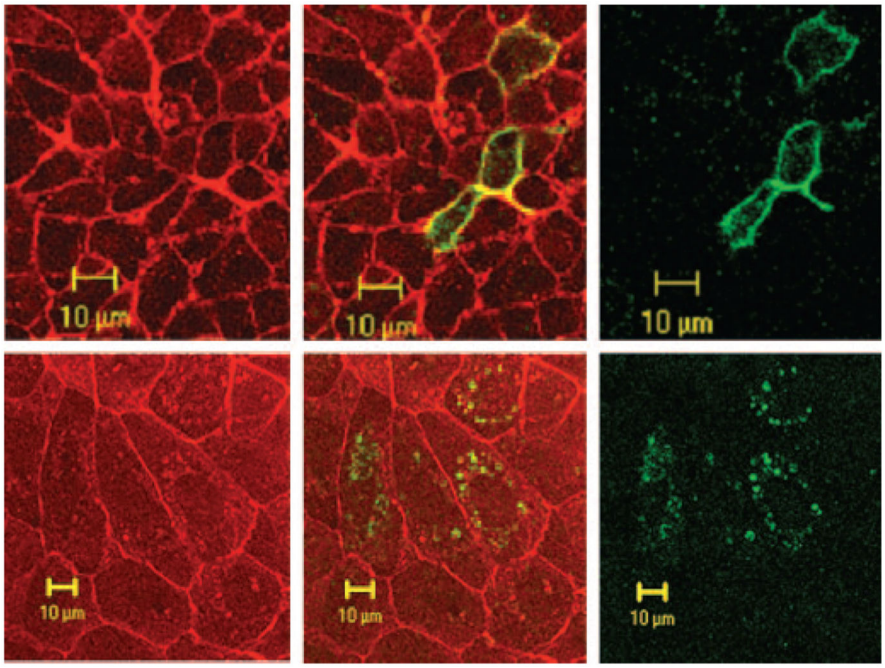

Figure 4.

Effect of mitogen activated protein kinase (MAPK) inhibition on subcellular distribution of SLC26A7 in hypertonicity. (Top) Hypertonic medium without MAPK inhibitor. As indicated, SLC26A7 is targeted predominantly to the plasma membrane in a hypertonic environment. (Bottom) Hypertonic medium with MAPK inhibitor. MAPK inhibitor completely blocked the trafficking of SLC26A7 to the membrane. Red, phalloidin; green, SLC26A7-GFP.

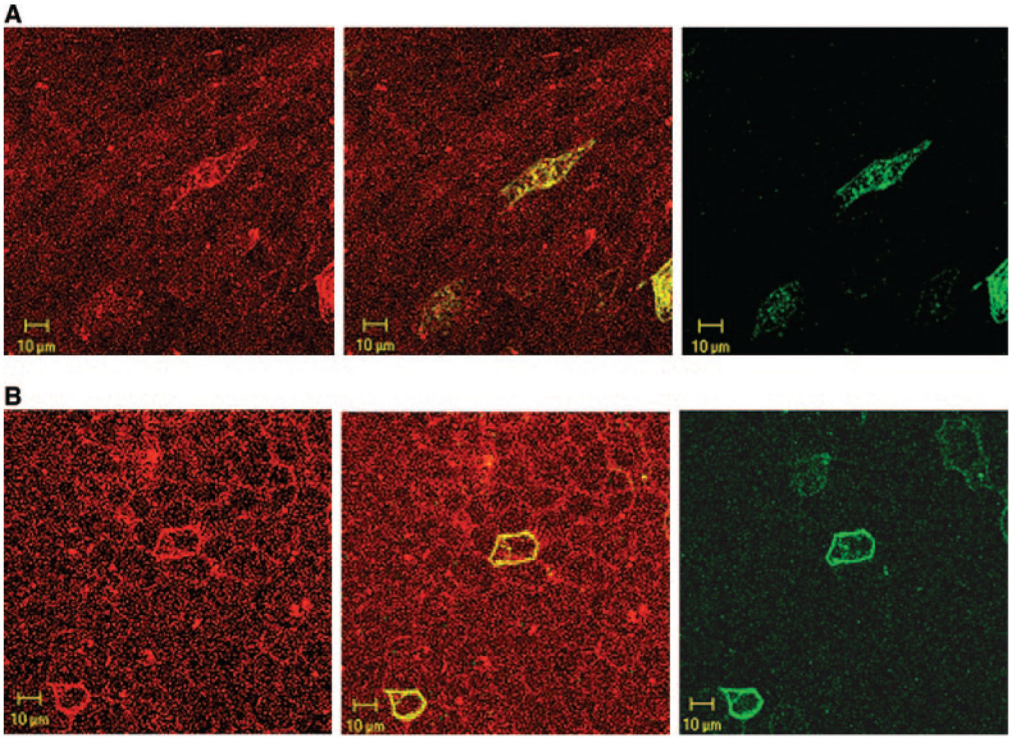

Figure 5.

SLC26A7 resides in recycling endosomes in MDCK cells. (A) Isotonic medium. As shown, SLC26A7 (right) and transferrin receptor (left) co-localize to the same intracellular compartments (middle: merged). (B) Hypertonic medium. SLC26A7 and transferrin receptor co-localize to the plasma membrane in hypertonic medium.

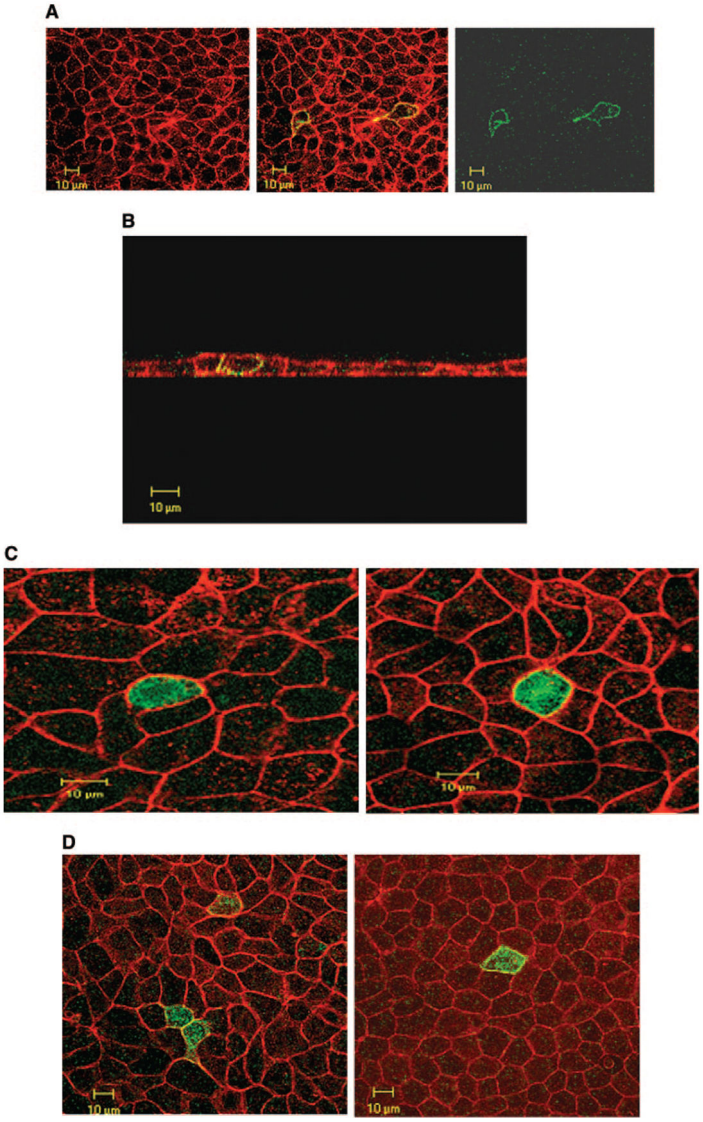

Figure 6.

Expression of SLC26A1, SLC26A7/A1 chimera, and truncated SLC26A7 in MDCK cells. (A) Expression of SLC26A1 in MDCK cells (Z-line image). SLC26A1 is expressed predominantly in plasma membrane, with no expression in the cytoplasm. (B) Subcellular distribution of SLC26A1 in isotonic medium (Z-stack images) indicates that SLC26A1 is localized to the basolateral membrane. Red, phalloidin; green, SLC26A1-GFP. (C) Expression of SLC26A7/A1 chimera in MDCK cells in isotonic and hypertonic media (Z-line image). SLC26A7/A1 chimera is expressed predominantly in the cytoplasm with some labeling in the plasma membrane (left, isotonic medium), and its distribution pattern does not change with increased osmolarity (right). (D) Truncated SLC26A7. As shown, the C-terminal–truncated SLC26A7 shows cytoplasmic distribution in isotonic medium (left). The truncated SLC26A7 remained predominantly in the cytoplasm with faint expression in the membrane in hypertonic medium (right).

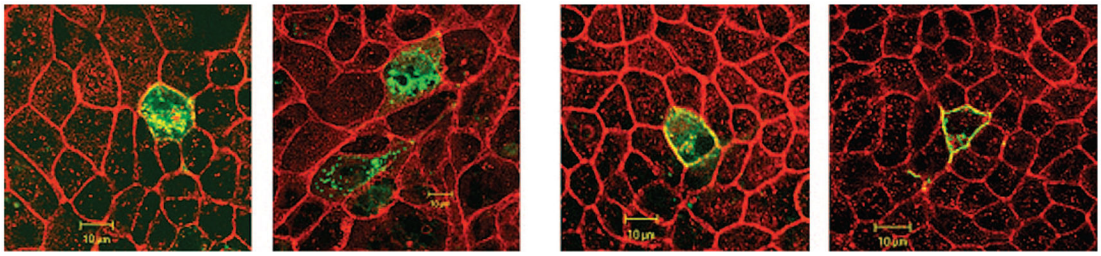

Figure 7.

Effect of potassium depletion on the subcellular distribution of GFP-SLC26A7 in MDCK cells. (Left) Normal potassium (4 mEq/L). (Middle two) Low potassium (2 mEq/L) for 2 and 16 h. (Right) Very low potassium (0.5 mEq/L) for 16 h. As demonstrated, SLC26A7 is expressed predominantly in punctate intracellular structures in normal potassium media (left) but is detected predominantly in the plasma in low-potassium medium for 16 h (right two). Second from left shows significant cytoplasmic localization with little membrane expression after short (2 h) incubation in low-potassium medium. Red, phalloidin; green, SLC26A7-GFP.

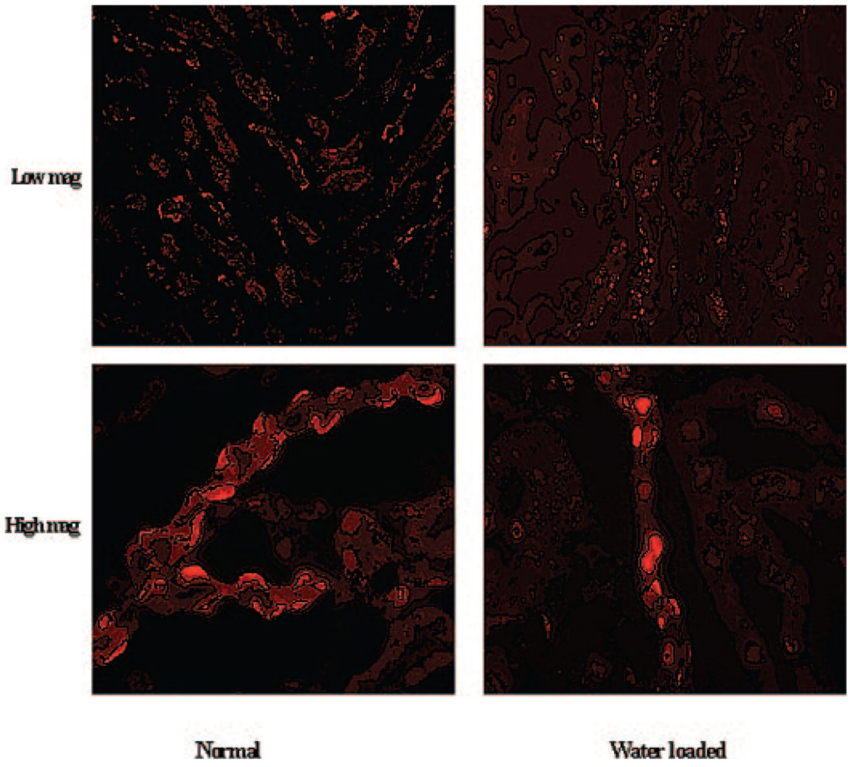

Figure 8.

Effect of water loading on SLC26A7 expression in rat kidney OMCD. (Top) Low magnification. (Bottom) High magnification. Immunofluorescence labeling demonstrates significant reduction in SLC26A7 expression on the basolateral membrane of OMCD in water-loaded rats (right) when compared with normal rats (left). The reduction in membrane expression was associated with reciprocal increase in SLC26A7 abundance in the cytoplasmic compartment.